Bulletin of the Seismological Society of America, Vol. 73, No. 2, pp. 615–632, April 1983

VARIABILITY IN GROUND MOTIONS: ROOT MEAN SQUARE ACCELERATION AND PEAK ACCELERATION FOR THE 1971 SAN FERNANDO, CALIFORNIA, EARTHQUAKE

BY MARTIN W. MCCANN, JR. AND DAVID M. BOORE

ABSTRACT

Data from the 1971 San Fernando, California, earthquake provided the opportunity to study the variation of ground motions on a local scale. The uncertainty in ground motion was analyzed by studying the residuals about a regression with distance and by utilizing the network of strong-motion instruments in three local geographic regions in the Los Angeles area. Our objectives were to compare the uncertainty in the peak ground acceleration (PGA) and root mean square acceleration (RMS_a) about regressions on distance, and to isolate components of the variance. We find that the RMS_a has only a slightly lower logarithmic standard deviation than the PGA and conclude that the RMS_a does not provide a more stable measure of ground motion than does the PGA (as is commonly assumed). By conducting an analysis of the residuals, we have estimated contributions to the scatter in high-frequency ground motion due to phenomena local to the recording station, building effects defined by the depth of instrument embedment, and propagation-path effects. We observe a systematic decrease in both PGA and RMS_a with increasing embedment depth. After removing this effect, we still find a significant variation (a standard deviation equivalent to a factor of up to 1.3) in the ground motions within small regions (circles of 0.5 km radius). We conclude that detailed studies which account for local site effects, including building effects, could reduce the uncertainty in ground motion predictions (as much as a factor of 1.3) attributable to these components. However, an irreducible component of the scatter in attenuation remains due to the randomness of stress release along faults during earthquakes. In a recent paper, Joyner and Boore (1981) estimate that the standard deviation associated with intra-earthquake variability corresponds to a factor of 1.35.

INTRODUCTION

Regressions of peak ground acceleration (PGA) against magnitude, distance, and site geology (e.g., Campbell, 1981; Chiaruttini and Siro, 1981; Joyner and Boore, 1981) are commonly used as the basis for the specification of design motions. The uncertainty in the predicted motions is often a key factor, especially for critical facilities. The observed uncertainties, as evaluated from the residuals about regression curves, are rather large, ranging from a factor of 1.45 (Campbell, 1981) to at least 1.9 (McGuire, 1978a; Joyner and Boore, 1981). (These uncertainties correspond to one standard deviation in the prediction of the peak acceleration.) Partly in the hopes of finding a parameter with less uncertainty, a number of investigations in recent years have considered alternatives to peak-value characterizations of strong ground motion. For example, response spectrum ordinates (McGuire, 1974), the root mean square acceleration (RMS_a) duration pair (Housner, 1975), and the Fourier amplitude spectrum of acceleration (Trifunac, 1976; McGuire, 1978b) have been proposed. The RMS_a is of particular interest, for it has a simple and direct relationship to seismological source models (Hanks, 1979), and, being an average statistic of the accelerogram, it would seem to be insensitive to isolated peaks that might contribute to the large uncertainty in peak acceleration predictions. Indeed, it can be shown that for a stationary Gaussian process, the RMS_a will have considerably lower variation than does the peak value. Simulation studies have verified this numerically for stationary and nonstationary signals. These arguments provided a sound basis to anticipate that the RMS_a might reduce the scatter in acceleration data. We find, however, that the RMS_a is not a more stable measure of ground motion than is PGA. One interpretation of this finding is that a large part of the scatter may be due to random multiplicative effects (such as laterally heterogeneous site amplification), such that both the PGA and RMS_a are affected equally.

We have attempted to isolate the sources of uncertainty in ground motion by studying the scatter of the PGA and RMS_a data about regressions with distance and for stations within regions of approximately $\frac{1}{2}$ km radius. The concentration of instruments effectively removes the possible contribution to the variance due to differences in source-site azimuth and propagation path. We conclude that geologic and other influences near to the site, including building effects, contribute a significant component (as much as a factor of 1.3) to the scatter in attenuation. We infer from these conclusions that detailed site response analyses could reduce the uncertainty in ground motion prediction due to these components. However, a remaining uncertainty in attenuation is that component due to source effects. Since the prediction of stress release patterns during earthquakes is not within current capabilities, we consider that component of the scatter attenuation due to source effects to be irreducible.

Data

Two nonoverlapping subsets of data from the 1971 San Fernando earthquake were used in this study; an attenuation data subset and a local area data group (Table 1). For attenuation with distance, the data set selected by Boore *et al.* (1978) was adopted. The records were chosen to avoid an azimuthal or distance bias that might result in overpopulating the data set with stations from downtown Los Angeles. The distance was measured to the closest point of rupture on the fault, and the local geology was classified according to the rock and soil categories defined by Boore *et al.* (1978). Station distances ranged from 15 to 100 km, the latter distance being determined by the distance to the first nontriggered operational station. For the study of variability within a small geographic region, stations in areas 1, 2, and 3 of Hanks (1975) were used. None of the stations in the area data group were used in the distance regression study.

To avoid possible bias of the peak value due to data processing, peak horizontal accelerations were taken from volume I of the California Institute of Technology series, edited by D. E. Hudson (1969), of uncorrected time histories. The volume II corrected accelerograms of the same series were used in the RMS_a and duration computations. The maximum value of each parameter is provided in Table 1.

Calculation of RMS_a

An RMS measure of signal strength is most commonly used for stationary signals. Earthquake accelerograms, on the other hand, are obviously transient signals, and thus the significance of the RMS_a is not clear *a priori*. The argument in support of RMS_a is that an earthquake of significant size will produce strong shaking over a time interval equal to many cycles of the dominant motion. If this is so, a meaningful measure of the RMS_a can be obtained with appropriate choice of integration limits in the defining equation,

$$RMS_a = \left\{\frac{1}{T_2 - T_1}\int_{T_1}^{T_2} a^2(t)\, dt\right\}^{1/2}. \quad (1)$$

TABLE 1

DATA USED IN THIS STUDY

EERL No.	Station No.	Distance (km)	PGA (cm/sec/sec)	$RMS_a(H)$* (cm/sec/sec)	$RMS_a(M)$† (cm/sec/sec)	Duration (sec)
		Small Structures—Soil Sites				
G107	475	22.0	111.89	34.24	32.15	11.40
D058	135	23.0	212.98	60.70	73.33	5.60
J141	828	27.0	149.18	36.84	32.37	13.80
G114	262	32.0	147.22	39.69	36.74	12.80
F103	807	41.0	145.26	35.54	37.89	7.20
N191	411	54.0	42.20	10.29	5.80	61.80
O205	130	59.0	29.44	9.54	7.75	52.80
P222	272	62.0	26.50	10.30	7.13	54.40
F101	113	91.0	55.94	12.43	13.16	8.20
		Small Structures—Rock Sites				
G106	266	18.4	20.22	45.01	59.25	4.40
O198	141	19.4	184.51	54.26	48.64	12.56
J144	128	21.0	367.06	71.84	80.02	7.72
J142	126	24.0	196.29	34.84	36.98	8.84
J143	127	24.0	144.27	25.79	34.53	5.20
D056	110	26.0	328.79	62.21	60.80	15.08
M184	290	59.0	61.80	14.78	16.74	6.40
F102	1096	64.0	27.48	6.44	9.44	6.54
		Large Structures—Soil Sites				
H115	466	15.0	220.83	64.03	57.49	14.08
Q233	253	15.4	258.12	75.95	75.41	10.40
F088	122	16.5	268.92	80.72	101.25	5.40
G108	264	21.0	202.18	45.70	56.68	4.40
H121	482	22.6	118.76	36.24	37.17	9.00
D057	133	23.0	150.16	45.91	54.43	5.60
D062	181	26.5	144.27	45.44	52.67	6.60
F086	288	33.0	108.94	30.21	24.84	17.00
H118	244	36.0	34.35	11.76	9.67	44.80
P231	247	37.0	44.17	12.09	10.33	30.40
S267	229	37.0	67.72	16.02	15.69	18.60
O204	131	58.0	27.48	7.00	6.88	49.20
N196	132	58.0	37.30	13.85	9.95	38.80
H124	476	58.0	39.26	12.29	9.42	23.40
M180	472	66.0	32.39	9.80	5.62	53.80
F087	281	70.0	28.46	9.59	5.38	78.60
P220	114	78.0	35.33	11.01	6.24	60.60
O206	274	93.0	46.13	11.12	11.32	10.00
		Area Data Groups				
E075	208		139.37	41.85	38.41	13.00
F083	199		178.62	50.27	59.30	6.40
J148	431	46‡	114.83	38.55	38.21	10.40
P217	196		119.74	32.45	30.03	13.00
S265	202		129.55	31.89	32.08	10.40
S266	211		163.90	39.97	37.78	10.60
C054	157		147.22	35.34	43.02	6.00
F098	175		149.18	41.54	50.84	5.80
F098	166		247.33	47.62	55.74	5.80
G112	163	48‡	104.03	28.76	32.13	7.20
K157	154		175.68	40.10	47.64	6.00
K159	170		211.99	66.66	72.50	7.40
R253	160		251.25	51.87	64.22	5.80
D059	187		160.96	38.57	44.03	7.00
R249	184		91.28	26.76	54.48	6.40
I134	425	45‡	101.09	31.40	35.29	7.20
I131	455		198.25	46.56	49.56	7.20
N188	440		126.61	44.20	29.85	6.80

* McGuire and Hanks (1980).

† McCann (1980).

‡ Hypocentral distance from Table 3.

Because it is not clear what values of T_1 and T_2 are best to use for a transient signal, we do the computations using two widely different approaches for determining T_1 and T_2. One, based on McCann (1980), determines T_1 by forming the cumulative RMS_a on the time-reversed accelerogram and noting where the cumulative RMS_a starts a steady decrease. The upper limit T_2 (and thus the value of RMS_a) is found by applying the same procedure to the nontime-reversed acceleration time history, starting at T_1. For the San Fernando data, this procedure gave durations ranging from 4.40 to 78.60 sec (see Figure 1 for examples of extreme cases and an average case). The other procedure we use to compute the RMS_a follows McGuire and Hanks (1980): T_1 is the time of the S-wave arrival and $T_2 = T_1 + 10$ sec, where the faulting duration is taken to be 10 sec for all records. The difference in the duration measures is emphasized in Figure 2. In spite of the differences in duration, the RMS_a estimates overall are consistent (Figure 3). Carrying out the subsequent analyses in this paper using both procedures for estimating RMS_a is a means of ensuring that the results will not be adversely affected by the inevitable arbitrariness of defining the RMS_a of a transient signal. This is important, for the basis of the paper will be residuals of the computed values about a regression line or a mean value.

Relative Variation in RMS_a and PGA

Previous empirical studies of the RMS_a for the San Fernando earthquake (Bond *et al.*, 1980; McGuire and Hanks, 1980) have shown a correlation between RMS_a and PGA. However, neither study explicitly considered the uncertainty in each ground motion parameter. One way to do this is by computing the residuals after removing the distance dependence obtained by fitting to the data the function

$$\log_{10} Y = A + B \log_{10} X \tag{2}$$

where Y is the ground motion parameter, and X is the distance. The standard deviation, $\sigma_{\log_{10} Y}$, of the residuals of the logarithmic random variable, provides a direct measure of the uncertainty in each parameter. The analysis was applied to the set of data recorded in small buildings on rock and soil sites (Table 2, Figure 4). A separate analysis showed no significant difference between the rock and soil data sets; therefore, the combined set was used in order to reduce the uncertainty in the derived variance. The resulting logarithmic standard deviations of the RMS_a residuals (0.16 and 0.20 for the McGuire and Hanks and McCann durations, respectively) were not significantly different from that of the PGA residuals (0.19) for the same data set. Analysis of the area group data supports this conclusion (Table 4).

Components of Ground Motion Variability

The scatter in ground motions can be attributed to a number of causes. For example, we might break the total variance into five parts: that due to transmission; azimuth; gross geologic differences; local geologic variations; and building effects. Each of the five parts have individual elements contributing to the variance. For example, local geologic variations may consist of topographic changes, lateral heterogeneities, near-surface fractures, the location of the water table, etc. Similarly, the contribution to the variance due to building effects may be attributable to

FIG. 1. A comparison of three time histories and their cumulative RMS functions (McCann, 1980). The examples illustrate three cases in which the RMS_a estimates for the duration measures of McGuire and Hanks (1980) and McCann (1980) are similar, but the durations are for cases in which the method by McCann [T_D (M)] gives (a) a shorter duration, (b) the same duration, and (c) a longer duration than the constant measure of McGuire and Hanks [T_D (H)].

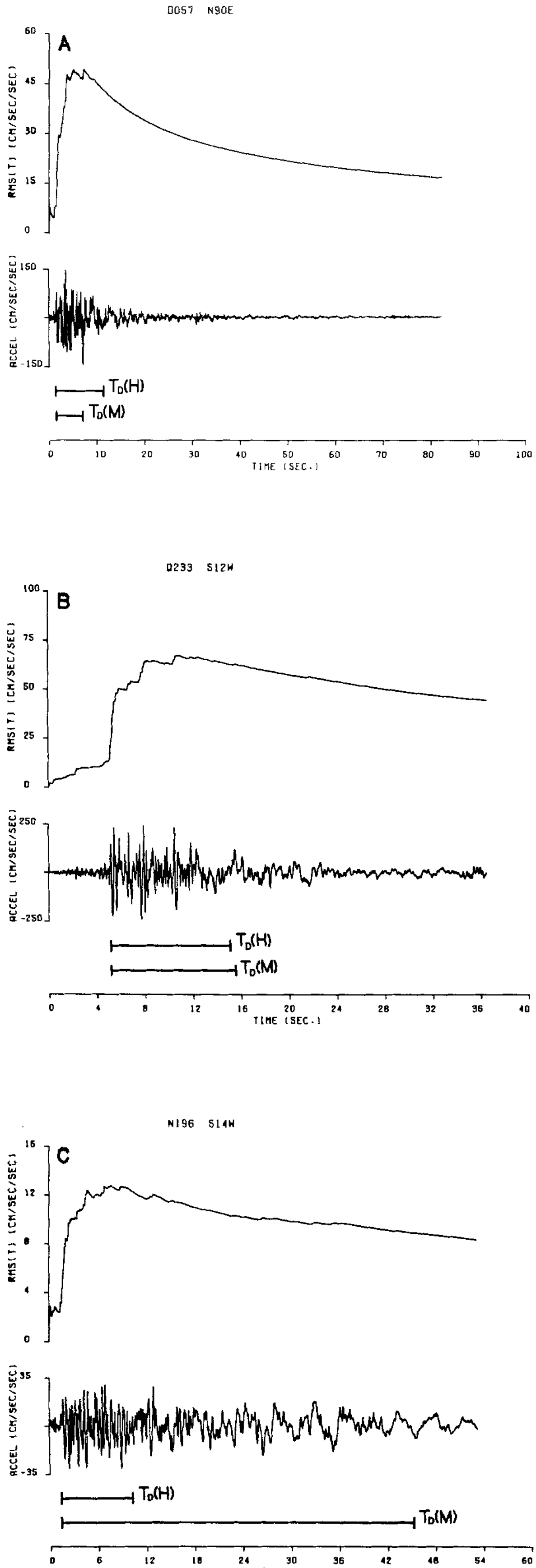
D057 N90E
A
RMS(T) (CM/SEC/SEC)
ACCEL (CM/SEC/SEC)
$T_D(H)$
$T_D(M)$
TIME (SEC.)
D233 S12W
B
RMS(T) (CM/SEC/SEC)
ACCEL (CM/SEC/SEC)
$T_D(H)$
$T_D(M)$
TIME (SEC.)
N196 S14W
C
RMS(T) (CM/SEC/SEC)
ACCEL (CM/SEC/SEC)
$T_D(H)$
$T_D(M)$
TIME (SEC.)

foundation type and size, the building mass, depth of embedment, and structure response feedback to the foundation. Ideally, we would perform a series of controlled experiments to provide a statistical sample sufficient to estimate systematic trends in the data in order to estimate the variance due to each of these sources. We have approximated several such experiments.

Hanks (1975) identified three areas with particularly dense concentrations of

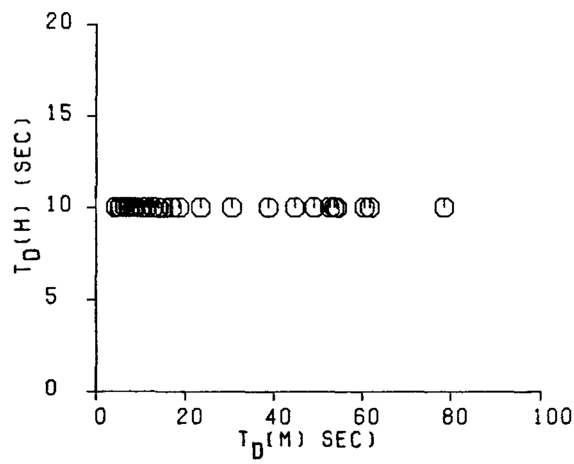

FIG. 2. A comparison of the duration estimates for the methods used in Figure 1, illustrating the large difference in their estimates of the strong-motion duration.

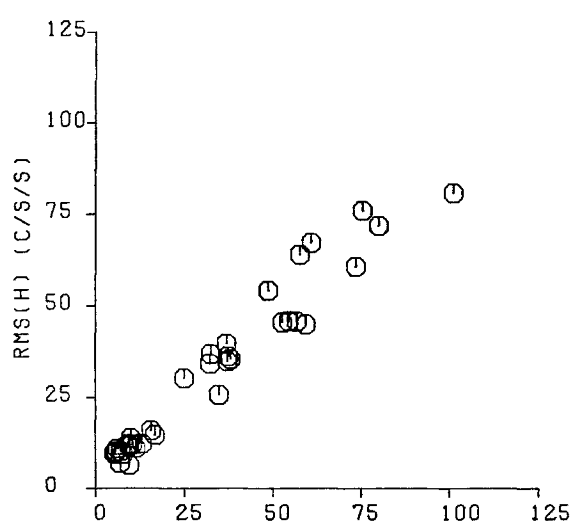

FIG. 3. The RMS_a estimates of McGuire and Hanks (1980) and McCann (1980) given in Table 1 are compared. The two methods give very similar estimates of the RMS_a.

instruments in the Los Angeles area (Table 3, Figure 5). Within each area, factors such as source-station azimuth, propagation path, and gross geologic features are effectively constant, removing in a gross way their contribution to the variance. Furthermore, we know something about the buildings and instrument locations in which the recordings were made, thus enabling us to estimate the building effects. We use the soil-site, large-building subset of the attenuation data to estimate the

TABLE 2
REGRESSION ANALYSIS RESULTS

Data Set	n*	RMS_a(H)			RMS_a(M)		
		A†	B†	$\sigma_{\log 10}$‡	A†	B†	$\sigma_{\log 10}$‡
RMS							
Large structures—soil sites	18	3.32	−1.27	0.15	3.73	−1.57	0.18
Small structures—soil sites	9	3.40	−1.27	0.17	3.54	−1.40	0.26
Small structures—rock sites	8	3.66	−1.49	0.19	3.51	−1.34	0.14
Small structures—rock and soil sites	17	3.56	−1.40	0.16	3.62	−1.43	0.20
PGA							
Small structures—rock and soil sites	17	4.16	−1.39	0.19			
Large structures—soil sites	18	3.40	−1.30	0.15			

* n is the number of data points.

† A and B are regression constants.

‡ $\sigma_{\log 10}$ is the standard deviation of the log-normal random variable or the logarithmic standard deviation. More specifically, it is used as follows

$$Y_p = Y_m \times 10^{\pm \alpha \sigma_{\log 10}}$$

where

Y_p = predicted value of Y at a probability of not being exceeded
Y_m = median value of Y
α = a constant based on the selected probability of not being exceeded.

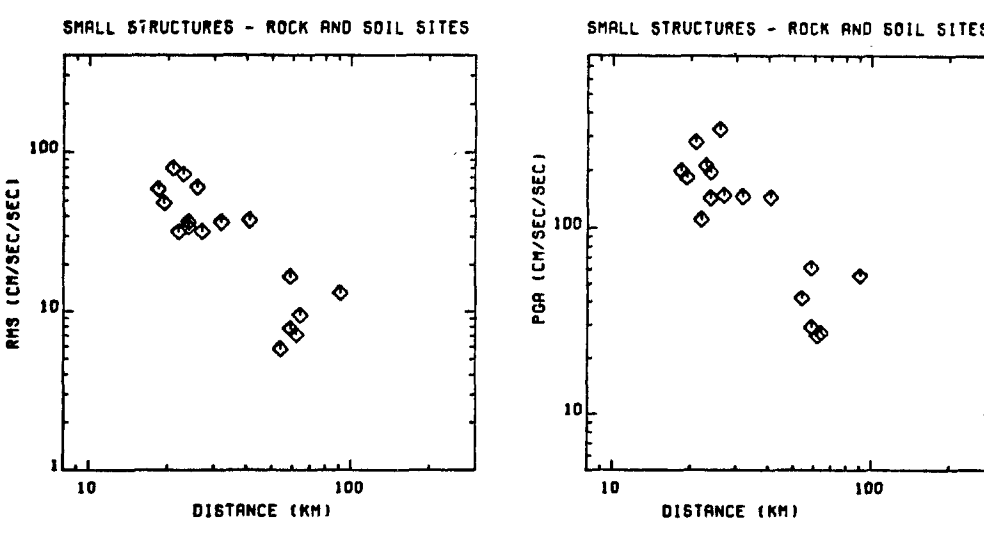

FIG. 4. Data recorded in small buildings on rock and soil sites for (a) RMS_a and (b) PGA data versus distance. The RMS_a values plotted in (a) are those using the method suggested by McCann (1980). Results of the regression analysis are given in Table 2.

TABLE 3

STATION DATA*

Sequence No.	EERL No.	Station	Instrument Depth (m)	Bldg. Stories	Length/ Width (m)	Soil Condition† (A)‡	(B)§	(C)¶
		Area 1: $R = 46$ km, $\phi = 167°$						
1	F083	Los Angeles, 3407 W. Sixth St.	1.5	11	26/44	1	0	0
2	E075	Los Angeles, 3470 Wilshire Blvd.	4.6	11	66/34	0	0	0
3	P217	Los Angeles, 3345 Wilshire Blvd.	3	12	29/48	0	0	0
4	J148	Los Angeles, 616 S. Normandie Ave.	3	17	50/18	—	1	0
5	S266	Los Angeles, 3550 Wilshire Blvd.	3	21	73/32	0	0	0
6	S265	Los Angeles, 3411 Wilshire Blvd.	16.8	31	98/229	1	1	1
		Area 2: $R = 48$ km, $\phi = 161°$						
1	F089	Los Angeles, 808 S. Olive Ave.	0	8	36/98	0	0	0
2	F098	Los Angeles, 646 S. Olive Ave.	1	8	47/43	0	0	0
3	K159	Los Angeles, 750 S. Garland Ave.	0	8	—	0	—	—
4	R253	Los Angeles, 533 S. Fremont Ave.	1.8	10	20/56	0	0	0
5	K157	Los Angeles, 420 S. Grand Ave.	7.5	17	41/49	0	—	—
6	C054	Los Angeles, 445 S. Figueroa St.	6.1	39	30/60	2	0	1
7	G112	Los Angeles, 611 W. Sixth St.	15	43	—	1	0	0
		Area 3: $R = 45$ km, $\phi = 186°$						
1	I131	Beverly Hills, 450 N. Roxbury Ave.	0	10	—	—	0	0
2	I134	Los Angeles, 1800 Century Park E.	11.3	15	54/30	0	0	0
3	N188	Los Angeles, 1880 Century Park E.	4	16	91/23	0	0	0
4	D059	Los Angeles, 1901 Ave. of Stars	13.6	19	34/74	0	0	0
5	R249	Los Angeles, 1900 Ave. of Stars	14.2	27	63/33	0	0	0

* Modified from Hanks (1975).

† The soil condition is rated as: 0, alluvium; 1, stiff; 2, rock.

‡ McGuire and Hanks (1980).

§ Trifunac and Brady (1975).

¶ Duke *et al.* (1972).

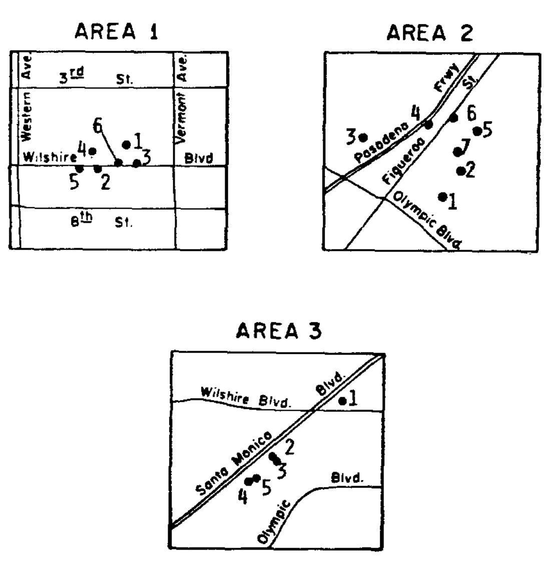

FIG. 5. The locations of the recording stations in areas 1, 2, and 3 in the Los Angeles area (modified from Hanks, 1975). The stations are numbered according to the sequence numbers in Table 3.

uncertainty introduced by propagation path (the variations in azimuth are not a factor, as all but one station are within the range 143° to 190°). The area group data and the attenuation data subset thus allow us to evaluate, in an approximate way, the contribution of three factors to the observed variability: propagation path (P); local effects (L); and building effects (B).

Hanks (1975) noted the strong amplitude and phase coherence of the ground displacements across the three local areas. The waveforms were independent of recording instrument, building size, record length, and triggering time. Accelerograms for stations within each area also show a strong phase coherence (Figure 6). In spite of this, there is considerable variation in the amplitudes, as the logarithmic standard deviations of both the RMS_a and PGA suggest (Table 4). Figure 7 shows the individual data points by area grouping; the numbers are keyed to Table 3 and increase with building height. For a direct comparison of the scatter in each parameter, Figure 8 shows the data normalized by their median value. As with the attenuation data group, we observe that the RMS_a residuals are not appreciably

TABLE 4

SUMMARY OF AREA DATA*

Area	Parameter	Median	$\sigma_{\log 10}$
	PGA	138.24	0.13
1	RMS_a (H)	38.91	0.11
	RMS_a (M)	38.73	0.17
	T_d (M)	10.52	0.15
	PGA	180.38	0.19
2	RMS_a (H)	43.85	0.18
	RMS_a (M)	51.58	0.17
	T_d (M)	6.27	0.07
	PGA	132.70	0.21
3	RMS_a (H)	37.10	0.15
	RMS_a (M)	42.08	0.16
	T_d (M)	9.92	0.03

* Units of median values are all in centimeters/second^2 except for T_d (M), which is in seconds.

different from the PGA residuals. Part of the scatter is due to the systematic effect of building size.

To investigate the possible contribution of building effects to the scatter, we chose the depth of instrument embedment as the variable having the most direct influence on ground motion. These influences include the reduction in ground motion amplitudes with depth below the free surface, and the effects of increased soil-structure interaction with increasing depth of embedment (Seed and Lysmer, 1980). Using the building height as the independent variable gives similar answers; this is not surprising, given the correlation between building height and number of stories below grade (Figure 9). There are, as others have suggested (Crouse, 1976; Campbell, 1981), other variables related to building size that influence the ground motion. Embedment depth was chosen because we believe it to be the most significant variable.

To determine the depth of instrument embedment, we have utilized a number of resources (U.S. Department of Commerce, 1973; U.S. Geological Survey station files; Crouse, 1976), including a visit to 15 stations to verify the instrument location. Without detailed engineering drawings, it was not possible to obtain for every station a direct estimate of the depth of instrument embedment in meters below grade.

Therefore, in a number of cases, where a depth in terms of the number of stories below grade was known, a value in meters was determined assuming there are 3 m per basement level.

In Figure 10, the data from the area data groups are shown versus instrument depth in meters below grade; a clear dependence on embedment depth can be seen. The observation of reduced amplitudes in strong motion records due to building or

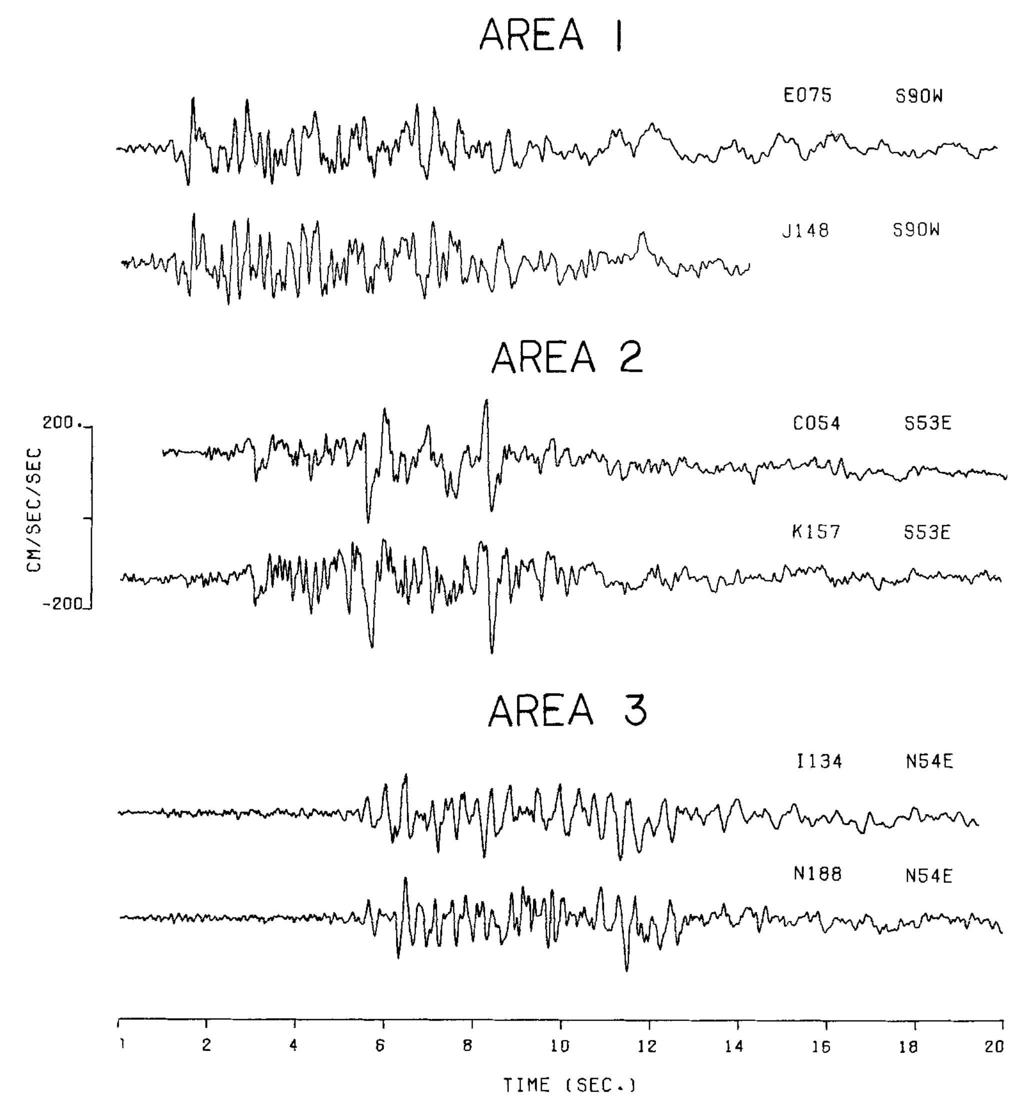

FIG. 6. Pair of accelerograms for each area in Figure 5. The waveforms show an obvious coherence in phase; however, differences in amplitude can be recognized.

foundation effects is not new. A number of empirical studies have identified instances where the motions observed on a structure foundation or a free-field station embedded to some depth, significantly influences the measured amplitudes (Crouse and Jennings, 1975; Crouse, 1976; Seed and Lysmer, 1980; Darragh and Campbell, 1981). Using the network of strong motion stations in the Los Angeles area, we are able to identify a systematic trend over a wider range of embedment depths than

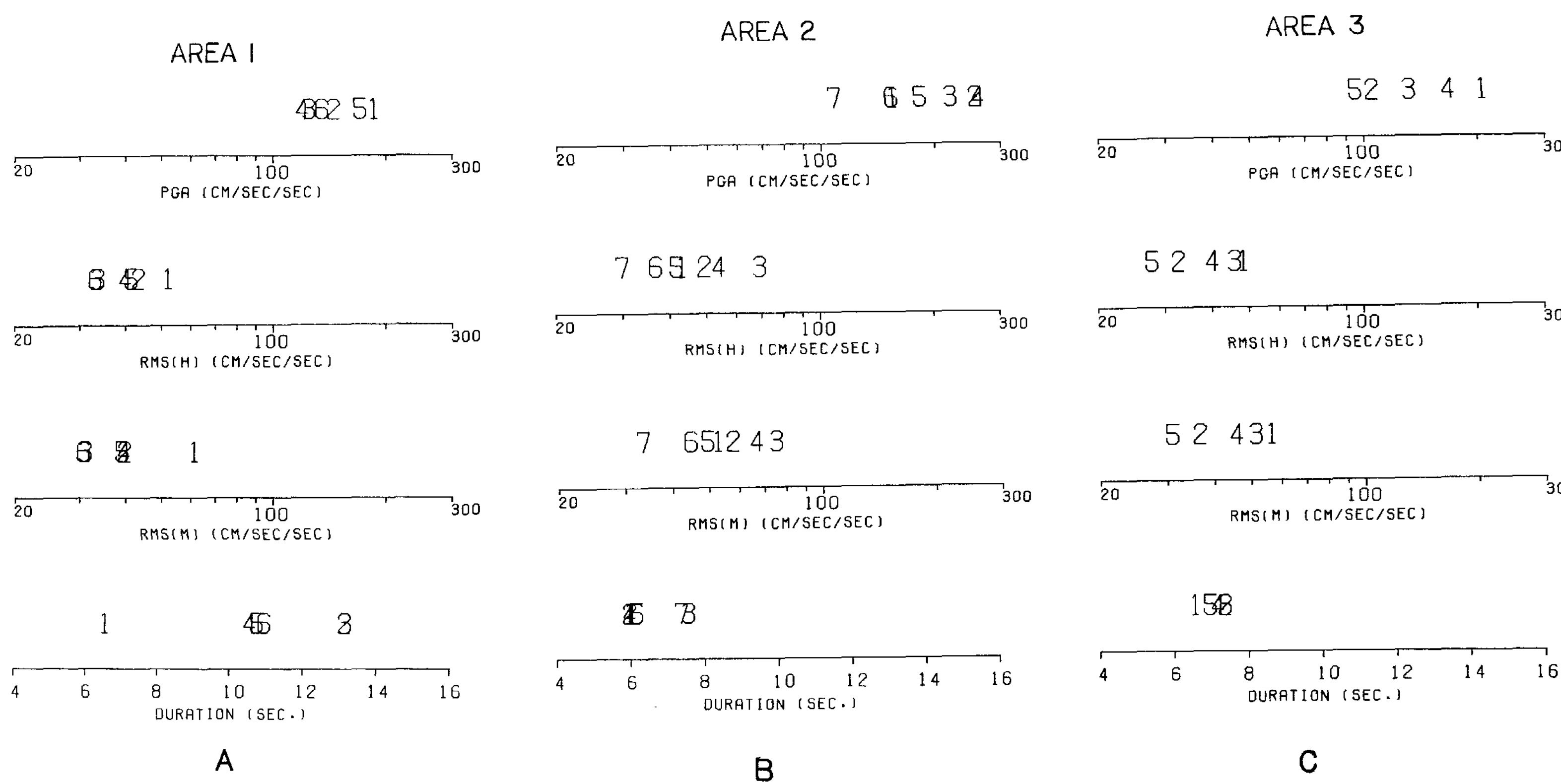

FIG. 7. PGA, RMS_a (for both measures of duration), and the duration estimated by McCann (1980) for the three areas in Los Angeles, (a) area 1, (b) area 2, and (c) area 3. The maximum value of the two horizontal components is plotted. Note the comparable scatter in the PGA and RMS_a.

was possible in most previous studies. To remove this systematic effect from the scatter in ground motions, a function of the form

$$y = c_0 + c_1 H + c_2 d_1 + c_3 d_2 \pm \sigma_L \tag{3}$$

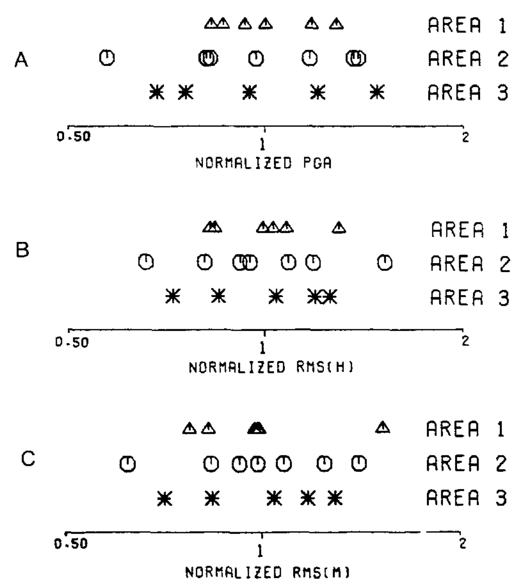

FIG. 8. The PGA data and RMS_a estimates in each area are normalized by their median values and plotted on the same scale, (a) PGA, (b) RMS_a (H), and RMS_a (M). This plot provides a direct comparison of the scatter in the estimates of the RMS_a and the PGA.

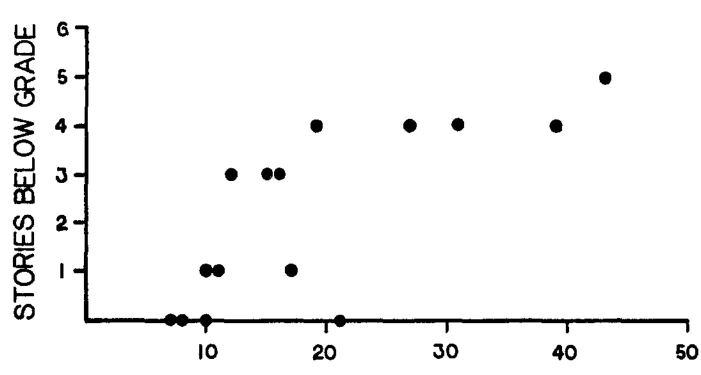

FIG. 9. Stories below grade versus stories above grade for the three area data groups combined.

was fitted to the data, where y is the log variable (PGA or RMS_a), H is the instrument depth in meters below grade, d_1 and d_2 are binary variables equal to 1 for the data in areas 1 and 2, respectively, and zero otherwise. The terms d_1 and d_2 serve to merge the three area data groups to a single subset that is regressed against instrument depth below grade. Table 5 gives the regression results. Since other buildings effects may exist besides those accounted for by a regression on the depth of embedment, the residuals about this curve are assumed to provide an upper-

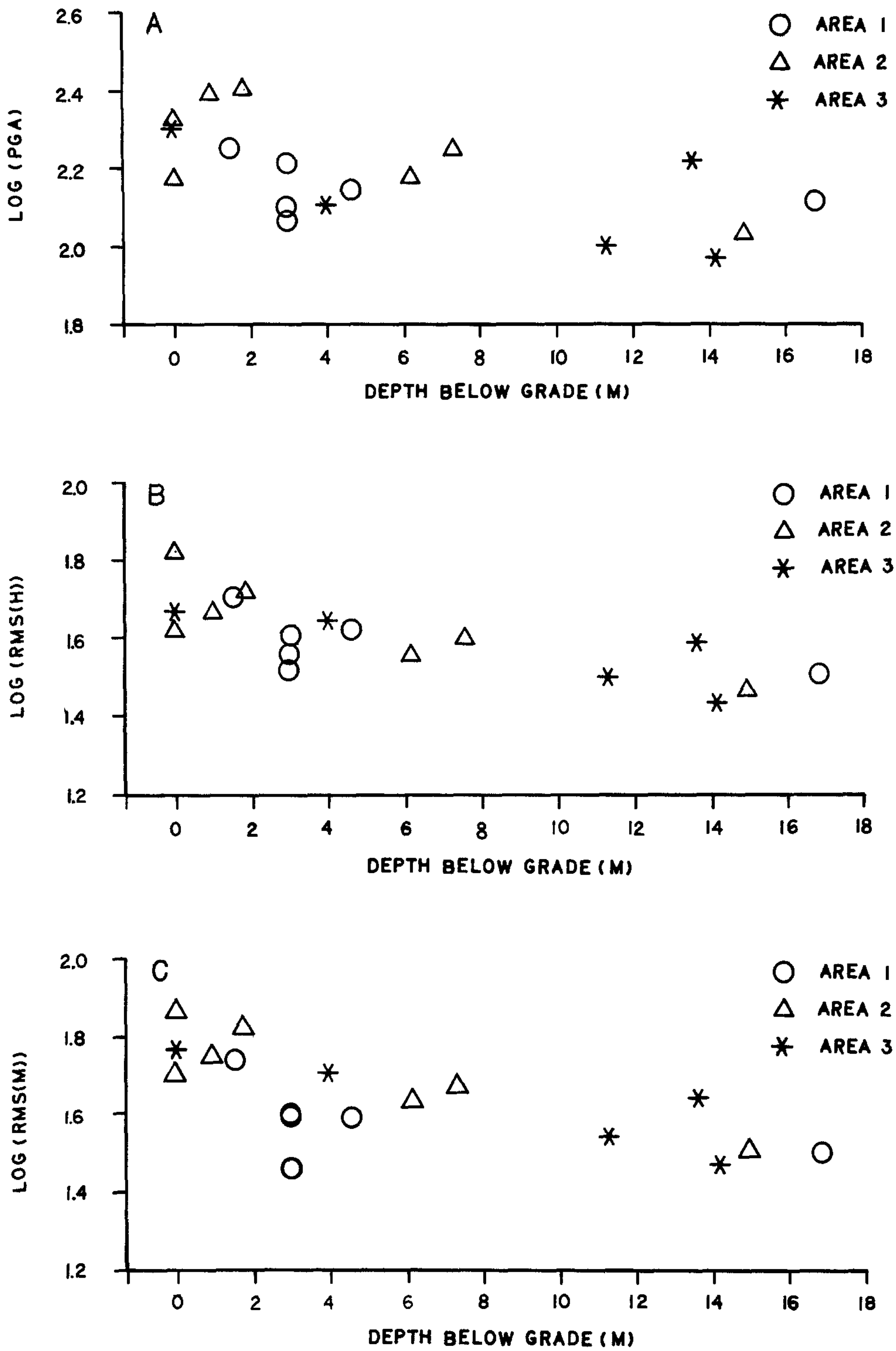

FIG. 10. PGA and RMS_a data versus embedment depth for the area data groups, (a) PGA, (b) RMS_a (H), and (c) RMS_a (M). Note the systematic decrease in the value of each parameter PGA, RMS_a (H), and RMS_a (M) with increasing depth of embedment. In the absence of information on the depth in meters below grade, a value in meters was determined assuming there are 3 m per basement level.

bound estimate of the contribution to the scatter due to local effects, σ_L, which is also given in the table.

For the attenuation data group, a function of the form,

$$y = c_0 + c_1 H \pm \sigma_{L\&P} \tag{4}$$

was fitted to the data, where y is the log residual about the distance regression, and H is the depth in meters below grade. The residuals about this regression curve provide an estimate of the contribution to the scatter due to local geology and propagation path, $\sigma_{L\&P}$. We note that for the attenuation data, an effect due to embedment depth was not identified. The main reason for this is probably that the range of embedment depths was much more limited than for the area group data. Assuming independence between local and propagation effects, it is possible to estimate the variance due to propagation ($\sigma_P{}^2$). This is achieved by combining the estimates of the variance due to local effects ($\sigma_L{}^2$) from the area data and that due to local and propagation effects ($\sigma^2_{L\&P}$) from the attenuation data. This has been done in the last column of Table 6.

TABLE 5

REGRESSION COEFFICIENTS

Attenuation Data	C_0	C_1			$\sigma_{L\&P}$
PGA	−0.01	0.00	—	—	0.15
RMS_a (H)	0.03	0.00	—	—	0.15
RMS_a (M)	0.00	0.00	—	—	0.18
Area Data	C_0	C_1	C_2	C_3	σ_L
PGA	2.22	−1.25E-2	−0.04	0.08	0.10
RMS_a (H)	1.68	−1.31E-2	−0.05	0.02	0.07
RMS_a (M)	1.74	−1.39E-2	−0.11	0.03	0.07

DISCUSSION

We have attempted in this study to test the idea that the RMS_a would have less scatter than the PGA, providing a parameter with lower uncertainty in predicted motions. We have also sought to isolate those components of uncertainty due to local site conditions, building effects, and propagation path. The standard deviations shown in Table 6 are the basis for the major conclusions of this paper.

The conclusions of our study are simply stated. First, contrary to our original expectations, the RMS_a is not a significantly more stable measure of ground motion than is PGA. Second, a significant scatter in both PGA and RMS_a exists for recordings in a limited spatial area, areas that we thought could generally be considered geologically uniform.

Before discussing the major conclusions of this study, we note that the data groups used in this investigation provide a unique, but not ideal, opportunity to study local variations in ground motions. The uncertainty in determining instrument depth below grade, the less than adequate distribution of station locations below grade in the attenuation data group, and the limited number of data points are limitations that make it impossible to unambiguously separate the influences of embedment depth, local effects, and propagation path. Furthermore, because of the limited number of data, we realize that the standard deviations may be uncertain enough that formal statistical tests will not necessarily support all the differences between them. However, even with these caveats in mind, we feel that there are systematic differences in the standard deviations shown in Table 6 that give some insight into the sources of the residuals.

We note that the RMS$_a$ using a fixed duration [RMS$_a$(H)] consistently leads to a slightly smaller variance in the measured RMS$_a$ than is obtained using the variable duration of McCann (1980) for the San Fernando earthquake data. Because they have a lower logarithmic standard deviation, we will use the RMS$_a$(H) residuals in the subsequent discussion. The RMS$_a$(H) uncertainty is slightly lower than the PGA (as expected from stochastic theory). The difference is probably not statistically significant; however, even if it were, a large reduction in the uncertainty of a ground motion estimate is not achieved by using the RMS$_a$ rather than the PGA.

TABLE 6

SUMMARY OF RESIDUALS*

	σ_T†	σ_L‡	σ_B§ $(= (\sigma_T^2 - \sigma_L^2)^{1/2})$
	Area Data		
PGA	0.12 (1.3)	0.10 (1.3)	0.07 (1.2)
RMS$_a$ (H)	0.10 (1.3)	0.07 (1.2)	0.07 (1.2)
RMS$_a$ (M)	0.11 (1.3)	0.07 (1.2)	0.08 (1.2)
	σ_T†	$\sigma_{L\&P}$‡	σ_P§$(= (\sigma_{L\&P}^2 - \sigma_L^2)^{1/2})$
	Attenuation Data (Large Structures—Soil Sites)		
PGA	0.15 (1.4)	0.15 (1.4)	0.11 (1.3)
RMS$_a$ (H)	0.15 (1.4)	0.15 (1.4)	0.12 (1.3)
RMS$_a$ (M)	0.18 (1.5)	0.18 (1.5)	0.16 (1.4)

* All numbers are rounded to two decimal places; factors (10^σ) are shown in parentheses.

† σ_T is the total logarithmic standard deviation about the median after merging the three area groups and about the distance regression for the area and attenuation data sets, respectively.

‡ σ_L, $\sigma_{L\&P}$ are the logarithmic standard deviations of the residuals remaining after regressing on embedment depths. The subscripts L and P suggest that the standard deviations are due to local and propagation effects.

§ σ_B, σ_P are derived standard deviations assuming independence of the various sources of scatter. For the area data, the total variance is assumed to consist of local effects (σ_L) and systematic effects due to embedment depth (σ_B). The entries in the last column of the attenuation data were derived by combining $\sigma_{L\&P}$ from the attenuation data set and σ_L from the area data set.

Our expectation of considerably reduced uncertainty in the RMS$_a$ is based in part on two simulation studies we performed to test this idea. In the first study, an ensemble of constant-duration stationary time histories were generated, while in the second the experiment was repeated with a suite of nonstationary signals. In both studies, the logarithmic standard deviation of the RMS was approximately 40 per cent below that of the peak value.

Our expectation of reduced variability in the RMS$_a$ was based on arguments that assume that the peak or extreme value and the RMS are parameters of the same random process. While our simulations perhaps serve as an adequate model for the unlikely case of many recordings at the same site for a suite of similar size earthquakes on the same section of the fault, the model is obviously not appropriate to explain the variation in motions for many recordings of one earthquake. If the site-to-site variations are solely due to random multiplicative effects acting on the same initial waveform, then we would expect the PGA and RMS_a will have similar logarithmic standard deviations. Multiplicative effects on the ground motion include radiation pattern, local heterogeneities in the stress release on the fault, and broadband site response functions. Thus in retrospect, it is not surprising that the PGA and RMS_a have similar scatter.

The relative uncertainty in the PGA and RMS_a measures of ground motion is the first concern of this paper; the second is the cause of scatter in the residuals. One of the most important reasons for conducting detailed studies of strong-motion data is to develop reliable tools for prediction. The large uncertainty in present predictions (as high as a factor of 1.9 at the one standard deviation level) almost demands that attempts be made to reduce this variability. To this end, we have conducted an admittedly less than ideal experiment to make quantitative estimates of three contributors to the variability: building embedment depth; local site response; and propagation path. We can summarize these results by giving the per cent contribution of each source of uncertainty to the total variance. For peak acceleration, we observe that building effects contribute approximately 20 per cent, while local geology accounts for 40 per cent of the total variance, and propagation path effects also contribute a 40 per cent share. For the RMS_a, there is some difference in that propagation path effects are the major contributor with about 60 per cent share of the total variance, while building effects and local geology each contributed an equal 20 per cent share. These percentages are relative to the total variance in the attenuation data set. Perhaps the most significant result is that in an absolute sense, the variation within a local geographic region is surprisingly large, even after removal of embedment effects. The standard deviation of this component corresponds to factors of 1.2 and 1.3 for RMS_a and PGA, respectively. The data were not adequate to estimate the scatter associated with azimuthal effects or interearthquake variability due to differences in stress release or types of faulting.

There are other observations of ground motion variability that corroborate our findings. The 1979 Imperial Valley earthquake provides evidence of the scatter observed in local regions. For data recorded at the El Centro Differential Array, the variability of peak accelerations for five stations with a maximum spacing of 214 m corresponded to a factor of 1.08. Regarding building effects on ground motions, Bycroft (1978) and McNeill (1982) point out that the instrument pad used in supposedly free-field installations can influence the ground motion. Their findings leave us to question whether *pure* free-field motions are in fact attainable, as there will be to one degree or another instrument pad and/or embedment effects.

A theoretical wave propagation study of peak ground motion in a layered earth model by Herrmann and Goertz (1981) suggests that variability in high-frequency ground motions should be expected, even for laterally uniform materials. Their studies, which provide an estimate of the variability due to propagation path and azimuthal effects for peak acceleration, indicate a range at the one standard deviation corresponding to factors of about 1.3 to 1.8.

Prediction of local site effects, including building influences, offer the most hope in reducing the variance in predicted ground motions. Although we were dismayed to find large variations in the PGA and RMS_a within circles of 0.5 km radii—areas that we thought would have reasonably uniform geologic properties—subsequent discussions with a geologist familiar with the areas revealed that many factors do exist that could produce variations in high-frequency motions. These include the presence of ravines, lateral changes in thickness and shear wave velocity of the near-surface, young sediments, and structural complexities due to faulting in area 3 (J. Tinsley, oral communication, 1982). Although often not practical, these and other factors could be identified by intensive geological and geophysical studies, including drilling and trenching. Empirical calibration of the site response, using ongoing seismicity as energy sources, is another possibilty.

There is less hope that the other components of variation could be predicted, although a case could be made that gross propagation path differences could be accounted for. The limitations of this lie in the ability to precisely know the character of the transmission path at wavelengths of interest. To the extent that these investigations of the site and the propagation path could be carried out, there remains that component of scatter in ground motion due to source effects. Although advances in our understanding of the seismic source have been made in recent years, it is still beyond our current capabilities to predict the character of stress release during a seismic event. Thus, we feel that the component of the scatter in regression analyses associated with the earthquake source can be considered irreducible. In a recent paper, Joyner and Boore (1981) estimate that the standard deviation associated with intra-earthquake variability corresponds to a factor of 1.35.

ACKNOWLEDGMENTS

We thank T. C. Hanks and W. B. Joyner for their thoughtful comments which led to significant modifications of the original manuscript and E. Ethridge, R. Maley, and J. Nielson for their assistance in gathering station data. The partial support of the National Science Foundation provided under Grants ENV77-17834 and PFR 809-06471 is gratefully acknowledged by the first author.

REFERENCES

Bond, W. E., R. Dobry, and M. J. O'Rourke (1980). A study of the engineering characteristics of the 1971 San Fernando earthquake records using time domain techniques, Report No. CE-80-1, Dept. of Civil Engineering, Rensselaer Polytechnic Institute, Troy, New York.

Boore, D. M., A. A. Oliver, III, R. A. Page, and W. B. Joyner (1978). Estimation of ground motion parameters, *U.S. Geol. Surv., Open-File Rept. 78-509.*

Bycroft, G. N. (1978). The effect of soil-structure interaction in seismometer readings, *Bull. Seism. Soc. Am.* **68,** 823–843.

Campbell, K. (1981). Near-source attenuation of peak horizontal acceleration, *Bull. Seism. Soc. Am.* **71,** 2039–2070.

Chiaruttini, C. and L. Siro (1981). The correlation of peak ground horizontal acceleration with magnitude, distance, and seismic intensity for Friuli and Ancona, Italy, and the Alpine Belt, *Bull. Seism. Soc. Am.* **71,** 1993–2009.

Crouse, C. B. (1976). Horizontal ground motion in Los Angeles during the San Fernando earthquake, *Earthquake Engineering in Structural Dynamics* **4,** 333–347.

Crouse, C. B. and P. C. Jennings (1975). Soil-structure interaction during the San Fernando earthquake, *Bull. Seism. Soc. Am.* **65,** 13–36.

Darragh, R. B. and K. W. Campbell (1981). Empirical assessment of the reduction in free field ground motion due to the presence of structures (abstract), Eastern Section, Seismological Society of America, *Earthquake Notes* **52,** p. 18.

Duke, C. M., K. E. Johnson, L. E. Larson, and D. C. Engman (1972). The effects of site classification and distance on instrumental indices in the San Fernando earthquake, ENG-7247, Earthquake Laboratory, School of Engineering and Science, University of California, Los Angeles, California.

Hanks, T. C. (1975). Strong ground motion of the San Fernando, California earthquake: ground displacements, *Bull. Seism. Soc. Am.* **64,** 193–225.

Hanks, T. C. (1979). *b*-Values and $\omega^{-\gamma}$ source models: implications for tectonic stress variations along crustal fault zones and the estimation of high frequency strong ground motions, *J. Geophys. Res.* **84,** 2235–2242.

Herrmann, R. B. and M. J. Goertz (1981). A numerical study of peak ground motion scaling, *Bull. Seism. Soc. Am.* **71,** 1963–1979.

Housner, G. W. (1975). Measures of severity of earthquake ground shaking, Proceedings U.S. National Conference on Earthquake Engineering, EERI, Ann Arbor, Michigan.

Hudson, D. E. (1969). *Strong Motion Earthquake Accelerograms Digitized and Plotted Data*, vol. I, *Uncorrected Accelerograms*; and vol. II, *Corrected Accelerograms and Integrated Ground Velocity and Displacement Curves*, Earthquake Engineering Research Laboratory, California Institute of Technology, Pasadena, California.

Joyner, W. B. and D. M. Boore (1981). Peak horizontal acceleration and velocity from strong-motion records including records from the 1979 Imperial Valley, California, earthquake, *Bull. Seism. Soc. Am.* **71**, 2011–2038.

McCann, M. W. (1980). RMS acceleration and duration of strong ground motion, Technical Report No. 46, The John A. Blume Earthquake Engineering Center, Stanford University, Stanford, California.

McGuire, R. K. (1974). Structural response risk analysis, incorporating peak response regressions on earthquake magnitude and distance, Massachusetts Institute of Technology, Department of Civil Engineering, Report R74-15, Cambridge, Massachusetts.

McGuire, R. K. (1978a). Seismic ground motion parameter relations, *Proc. Am. Soc. Civil Eng. J. Geotech. Eng. Div.* **104**, 481–490.

McGuire, R. K. (1978b). A simple model for estimating Fourier amplitude spectra of horizontal ground acceleration, *Bull. Seism. Soc. Am.* **68**, 803–822.

McGuire, R. K. and T. C. Hanks (1980). RMS accelerations and spectral amplitudes of strong motion during the San Fernando earthquake, *Bull. Seism. Soc. Am.* **70**, 1907–1920.

McNeill, R. L. (1982). Some possible errors in recorded free-field ground motions (abstract), Eastern Section, Seismological Society of America, *Earthquake Notes* **53**, 90–91.

Seed, H. B. and J. Lysmer (1980). The seismic soil-structure interaction problem for nuclear facilities, Seismic Safety Margins Research Program, Lawrence Livermore Laboratory, UCRL-15254, Livermore, California.

Trifunac, M. D. (1976). Preliminary empirical model for scaling Fourier amplitude spectra of strong motion accelerations in terms of earthquake magnitude, source-to-site distance and recording site conditions, *Bull. Seism. Soc. Am.* **66**, 1343–1373.

Trifunac, M. D. and A. G. Brady (1975). On the correlations of seismc intensity scales with the peaks of recorded strong ground motion, *Bull. Seism. Soc. Am.* **65**, 139–162.

U.S. Department of Commerce (1973). San Fernando, California Earthquake of February 9, 1971, National Oceanic and Atmospheric Administration, Leonard M. Murphy, Scientific Coordinator, volume I, parts A and B.

Jack R. Benjamin and Associates, Inc.
444 Castro Street, Suite 501
Mountain View, California 94041
and
The John A. Blume Earthquake Engineering Center
Stanford University
Stanford, California (M.W.M.)

U.S. Geological Survey
345 Middlefield Road
Menlo Park, California 94025 (D.M.B.)

Manuscript received 14 April 1982